Research Article

Yuanfei Gao, Mohammad Heydari Vini, and Saeed Daneshmand*

Effect of nano Al_2O_3 particles on the mechanical and wear properties of Al/Al_2O_3 composites manufactured via ARB

https://doi.org/10.1515/rams-2022-0268 received April 06, 2022; accepted August 29, 2022

Abstract: This study first tried to fabricate $AA1060/Al_2O_3$ composites via the stir casting and accumulative roll bonding process. Then, the effect of nano Al_2O_3 Vol% on mechanical, wear, and microstructural properties of these kinds of composites have been investigated. An excellent particle distribution through the aluminum matrix has been achieved after the fourth cycle. Then, mechanical properties, wear resistance, and microstructural properties have been investigated. The results showed that the strength of these composites was enhanced and the elongation of samples decreased by higher alumina Vol% contents. Also, there is a significant increase in wear resistance by increasing alumina content in the Al matrix through the stir casting process.

Keywords: accumulative roll bonding, mechanical properties, metal matrix composites, wear resistance, wear test

1 Introduction

Nowadays, aluminum-based composites are popular in many industries similarly as electrical, vessels, chemical, aerospace, etc. due to having excellent properties such as light density, high mechanical properties, high wear, and corrosion resistance [1–8]. Usually high hardness value of alumina particles makes it a desirable additive for

* Corresponding author: Saeed Daneshmand, Department of Mechanical Engineering, Majlesi Branch, Islamic Azad University, Isfahan, Iran, e-mail: S.daneshmand@iaumajlesi.ac.ir, tel: +98-3152462103, fax: +98-3152464292

Yuanfei Gao: School of Chemistry and Pharmaceutical Engineering, Nanyang Normal University, Nanyang, Henan Province, China

Mohammad Heydari Vini: Department of Mechanical Engineering,

Mobarakeh Branch, Islamic Azad University, Mobarakeh, Isfahan,

Iran, e-mail: m.heydari@mau.ac.ir

utilizing as an emergent reinforcement in aluminum base composites [9-17]. Usually aluminum-based composites can be produced via several methods such as alloying laser techniques [18-20], plasma and highspeed oxygen fuel spray, and sputtering and high-energy milling techniques [21–23]. These techniques enhance the mechanical properties and wear resistance of Al-based composites by generating a hard coating on the Al matrix by sticking alumina particles through it. These particles are popular as reinforcing in MMCs due to having fantastic possessions such as high and abrasion resistance, degree of hardness, and melting point. To produce aluminumbased composites (AMMCs), stir casting usually is famous as a low-cost process for having the capability for high volume production and its simplicity. So, this process creates a low cavity (porosity) structure with an unvarying scattering of the additive particles through the metallic matrix [24-26].

Reviews on Advanced Materials Science 2022; 61: 734-743

Many forming processes through severe plastic deformation (SPD) processes are utilized to fabricate Al-based composites, such as accumulative roll bonding (ARB), cyclic extrusion compression [20], squeeze casting, spray forming [18,19], and powder metallurgy [27]. While cast MMCs usually have a desirable particle distribution through the metallic matrix, they have poor fracture toughness and ductility. So, processing of these kinds of composites via an SPD deformation technique is necessary [21]. So, these problems inspire the helping of manufacturing techniques such as ARB after the stir casting process, in this study. Saito was the first researcher who proposed the ARB for the first time in 1998 [23]. ARB is defined as cumulative rolling processes on multi-layered strips with the same primary dimensions which have been prepared. This process is not only a forming technique but also a bonding (as a branch of solid phase method of welding) process. For each ARB process, the reduction in thickness is 50% and will be repeated for all cycles. The main purpose of this study is to produce Al/alumina bulk composites by combined stir casting and ARB at 300°C and improve the mechanical properties with the homogenous spreading of alumina particles. It was tried to produce Al/alumina composite with unvarying dispersed alumina particles in the Al matrix and estimate the wear, microstructural, and mechanical properties such as hardness, strength, and elongation.

2 Experimental procedure

2.1 The stir casting process

The fully annealed primary material aluminum alloy 1060 is used for fabricating the experimental samples. Alumina particles as additive particles with an average grain size of 50 nanometers are used as reinforcement with a purity of 99%. Before the casting process, the additive particles were preheated at 400°C for 5 hours to diminish their humidity. The alumina particles with 0, 2.5,5 and 10 Vol% were put on the surface of the aluminum melt at 750°C, and this composition was rotated with a rotary speed of 650 rpm with the blowing of Argon gas to protect the melt from oxidation (Figure 1). The stir casting process allows the creation of a desirable bonding between aluminum and alumina particles which leads to decreasing the number of voids and cavities in the final composite matrix. The dimension of the final fabricated composite samples is $200 \text{ mm} \times 26 \text{ mm} \times 1 \text{ mm}$.

Brushing the surface of composite samples prior to the ARB process is necessary to create a desirable bonding between composite layers. Based on the film theory (one

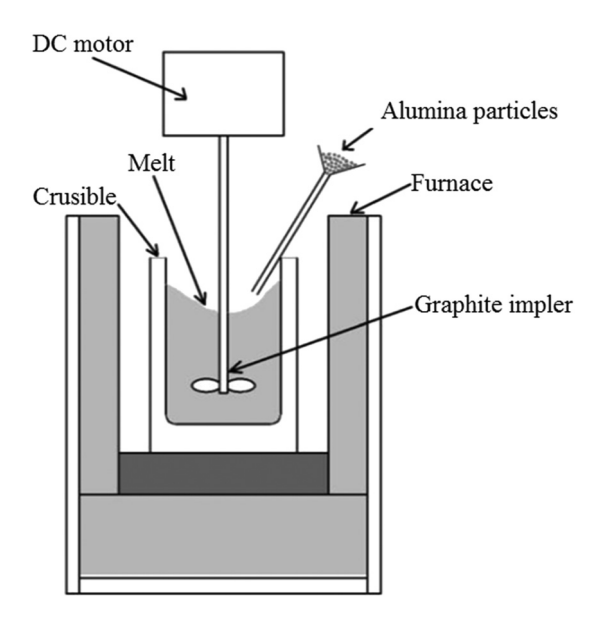


Figure 1: Diagram of the experimental setup secondhand in making of the cast AI/AI_2O_3 composites.

of the main theories to explain the solid phase method of welding), brushing the surface of composite samples before ARB allows to deliver a coarse surface which introduces a restricted shear during the forming process and disrupts the oxide layers. This disruption creates more cracks and allows the virgin metals to extrude along the cracks and toward the opposite composite layers which create metallic bonding [23].

2.2 ARB process

At the starting of the ARB process and to clean the contaminations and grease from the surface of composite samples, the samples were brushed and put in the acetone bath for 30 min. Then, the samples were heated at 300°C for 10 min, and the two strips were stacked against each other. In continuing, all the samples were rolled with a thickness reduction ratio of 50% (Figure 2). Then, the samples were halved and the surface preparation process was repeated for each cycle. According to Figure 3, adsorbed ions, greases, oxides, and dust subdivisions have surrounded the surfaces of samples. Using a 95 mm diameter stainless steel with 0.26 mm wire diameter and speed of 2,000 rpm, the sample strips were scratch brushed after degreasing in the acetone bath. So, surface cleaning before each cumulative rolling process is essential to generate an acceptable bonding.

To study the effect of Al_2O_3 Vol% on the wear and mechanical properties, The ARB was continued for up to four cycles to generate a desirable scattering of alumina subdivisions in the Al matrix. So, the ARB steps of the process are summarized in Table 1.

In order to set up the rolling process, a laboratory rolling machine with a capacity of 40 tones with a rotary speed of 60 rpm and a roll diameter 170 mm is used in this study. According to Figure 4 in order to supply the tensile test samples, ASTM standards E8M has been used. Also, standard ASTM-E384 with a 500 grams load for fifteen seconds was used as the Vickers hardness testing condition. The samples were prepared for wear test with $60 \, \mathrm{mm} \times$ $30 \text{ mm} \times 1 \text{ mm}$, and the test was performed by means of a "pin on disc" wear testing machine fitting into the fixture. The wear parameters were 500 s test time, 20 N load, and 1 m·s⁻¹ velocity. Wear tests were conducted using a "pin on disc" wear testing machine, with the $60 \, \mathrm{mm} \times 30 \, \mathrm{mm} \times 10^{-3} \, \mathrm{mm}$ 1 mm samples used. As the wear pin, a stainless steel pin containing 30 mm long and 8 mm in diameter was used. Also, the worn surface of samples was observed via scanning electron microscope (SEM).

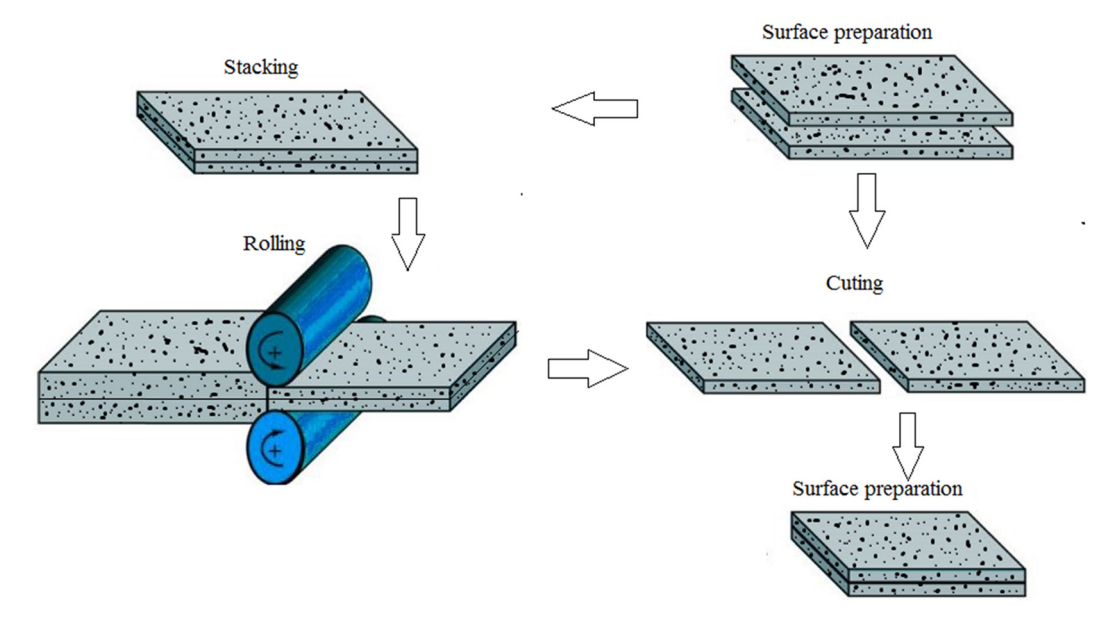


Figure 2: Graphic diagram of the ARB.

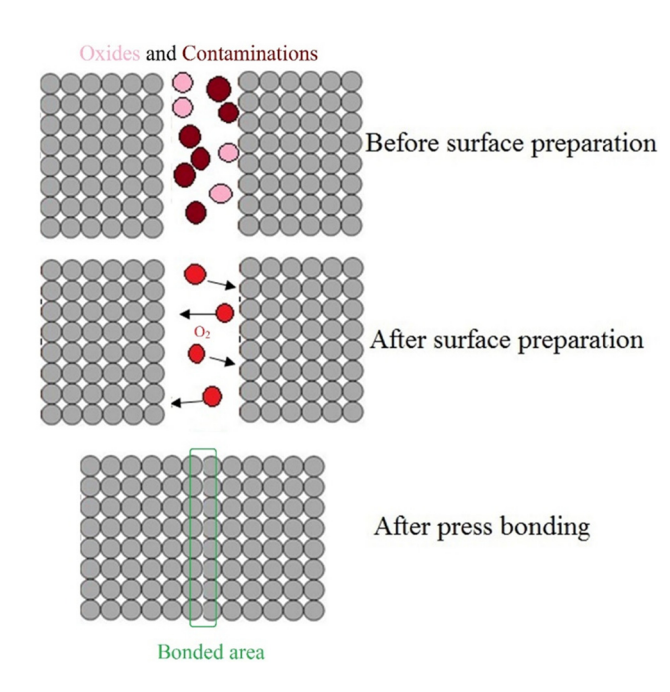


Figure 3: Atomic arrangement of composite samples during the bonding during the ARB process.

3 Results

3.1 Alumina particles distribution

Figure 5 shows the SEM micrograph of composite layers after cycle No. 4. As shown in the figure, after the fourth cycle, the alumina particles have a uniform distribution inside the composite matrix, and because of this, for investigating the effect of alumina Vol%, all samples have been fabricated after four cycles of ARB. In other words, by increasing the cumulative rolling up to four cycles, the distance between alumina particles increases which leads to disruption of alumina clusters and generation of uniform particle scattering.

3.2 Mechanical properties

Having different alumina volume contents fabricated after four cycles, tensile tests have been carried out for MMC

Table 1: ARB process steps for fabrication of Al/alumina composites

No. of steps	Rolling temperature (°C)	No. of composite layers	Reduction in cycles (%)	Composite layer thickness (µm)	Final reduction (%)	Plastic strain
1	300	2	50	1,000	50	0.8
2	300	4	50	500	75	1.6
3	300	8	50	250	87.5	2.4
4	300	16	50	125	93.7	3.2

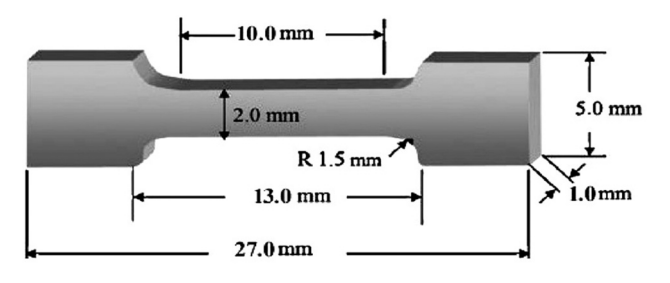


Figure 4: Dimension of the tensile test specimen.

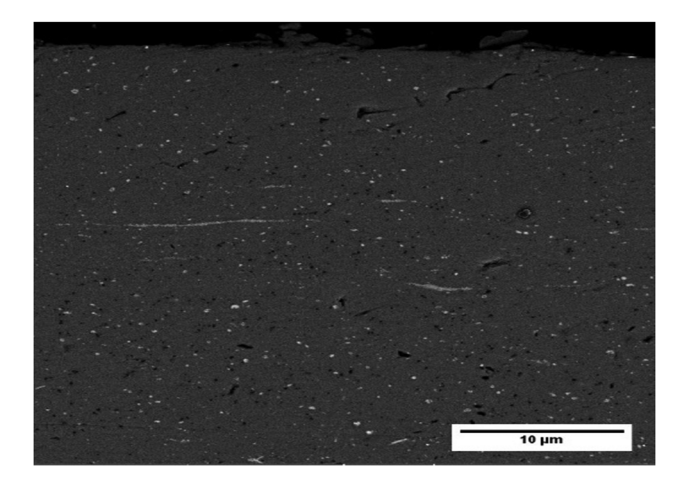


Figure 5: SEM cross-section of the composite sample after the fourth cycle reinforced with 10 Vol% of alumina.

samples (Figure 6). The flow stress rapidly reaches its maximum value by increasing the plastic strain. The enhancement

of the mechanical properties was achieved by increasing the alumina content (Figure 6). According to Figure 7, the tensile strength of the ARBed MMCs is 127.75 and 178 MPa for monolithic samples and samples produced with 10 Vol% of alumina content registering 39.3% improvement. Strain hardening around the alumina particles during the rolling process activates the slip systems which generates further dislocations close the particles and decreases the flexibility of dislocations [19]. Also, because the ARB has been done in this study is a warm forming process, there is grain refinement during all the ARB cycles. Both of them lead to improving in the strength and decreasing in the elongation of samples which decreases the bonding strength.

The elongation of samples decreases considerably at higher Al₂O₃ contents which attributed to the weak adhesion of particles agglomerations to the Al matrix (Figure 7). Always, alumina particle layers contain voids affecting the elongation reduction. The harder particles block the motion of Al grains which increases the dislocation density [28-31]. All of these effects reduce the elongation and enhance the strength of the AA1060/alumina composites. According to Figures 6 and 7, higher volume fraction of particles leads to more strain hardening around the particles. So, the tensile strength increases while ductility drops. The ductility of the ARBed MMCs is 4.28% (monolithic sample) and 1.8% (10% alumina), as shown in Figure 7. As mentioned before, reduction of dislocation mobility and work hardening lead to the creation of this behavior. As mentioned before, porosities in alumina layers reduce the elongation value. So, the reasons (mechanism) for

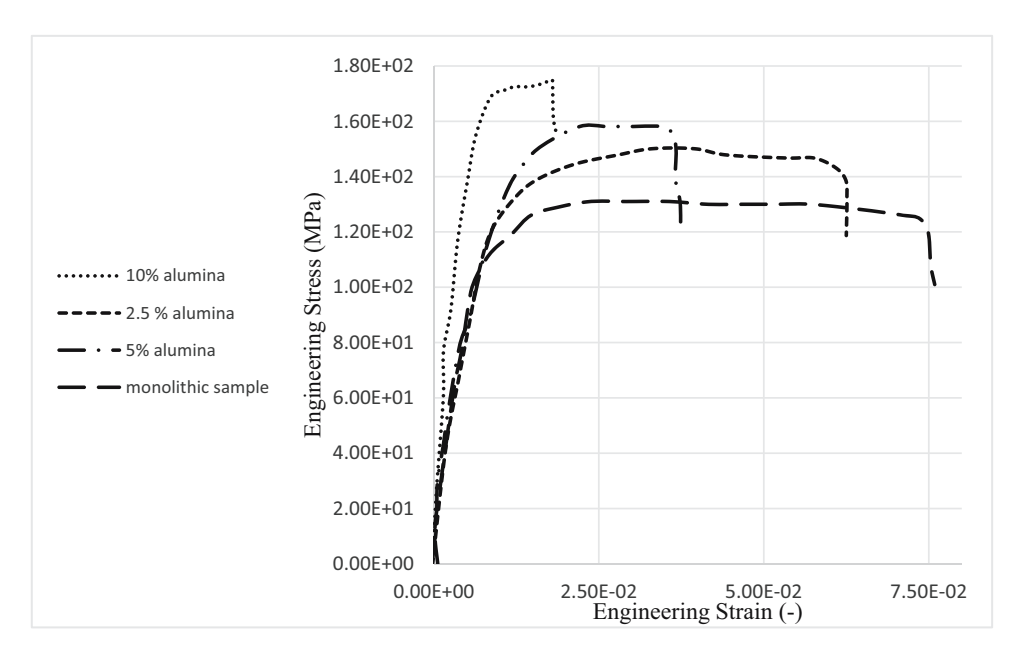


Figure 6: Engineering stress-strain curves of ARB-processed samples.

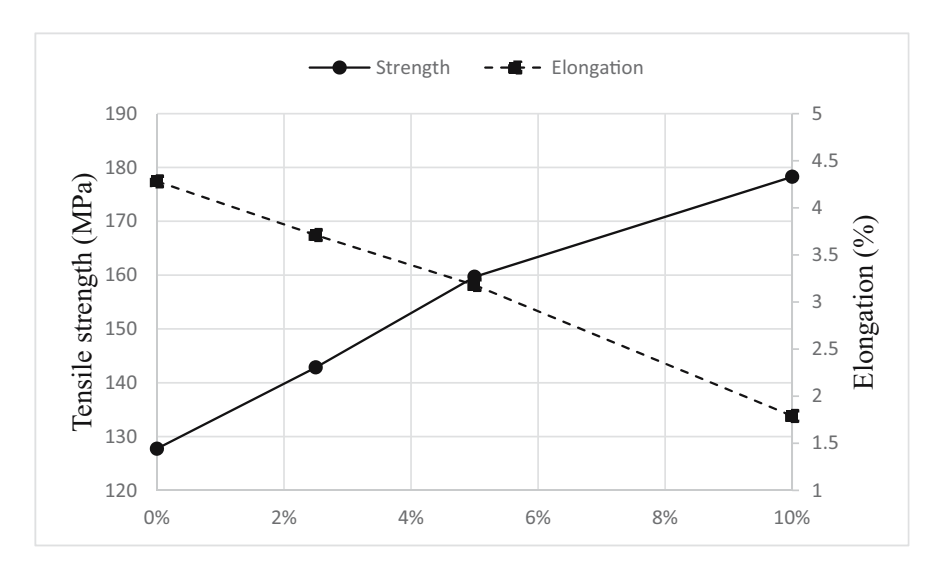


Figure 7: Tensile strength and elongation of composite samples vs alumina Vol%.

enhancing the elongation are (i) growing the uniformity of alumina subdivisions inside the aluminum matrix, (ii) increasing the bonding between the Al matrix and alumina particles which decreases the voids among them, and (iii) decreasing the agglomeration and dispersing them inside the metal matrix.

The toughness value drops considerably from $4.2\,\mathrm{J\cdot m^{-3}} \times 10^4$ (monolithic sample) to $2.7\,\mathrm{J\cdot m^{-3}} \times 10^4$ (10% alumina), which is due to the less mobility of dislocations and stress hardening (Figure 8). So, increasing the number of alumina particles as a barrier against the grain's movements in the AA1060 matrix decreases the elongation severely which reduces the toughness amplitude [27,32–34].

The hardness values of the samples after ARB increase (Figure 8). According to Figure 8, the average Vickers

hardness amount increases from 157.0 up to 167.0 which is about 5.70% enhancement. With increasing the content of particles, the first reason for increasing the hardness via forming processes is the generation of a fine grain structure due to the amount of plastic strain. This phenomenon leads to the growth of dislocation density which impedes the movement of grain boundaries and leads to increasing the initial work hardening [21,31]. The materials gain a certain steady-state density of dislocations by increasing the ARB cycles up to four cycles. In stage 2, the limited work hardening around the alumina particles is the main factor in increasing the hardness value. So, higher values of alumina particles inside the composite matrix generate more strain hardening, and as a result, the hardness improves.

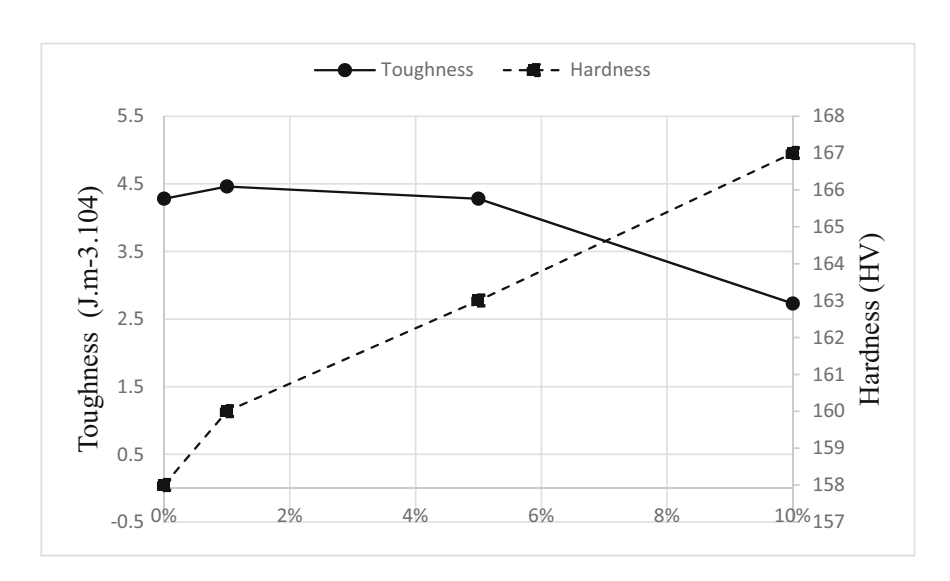


Figure 8: Variations of toughness and hardness vs alumina content.

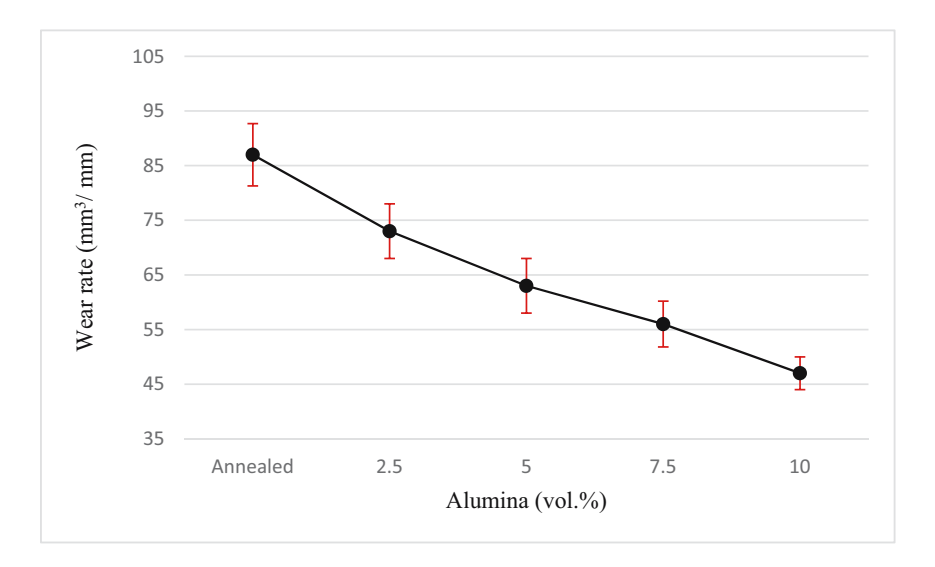


Figure 9: Wear rate in sliding wear for Al/alumina composite vs alumina volume content.

3.3 Wear test

Figure 9 shows the wear rate of composite samples versus alumina particles content fabricated via four cycles of ARB. As can be viewed in Figure 9, the most wear rate is for the monolithic composite sample (87 mm³·mm⁻¹). The least value for the wear test belongs to the sample fabricated with 10% of alumina (47 mm³·mm⁻¹). In the other words, the uniform distribution of alumina particles leads to the reduction of weight loss. This trend is due to the work hardening effect of the Al matrix and the dislocation strengthening mechanism around the alumina particles. Also, higher cycles lead to decreasing the porosities between alumina particles and aluminum base matrix which improves the bonding strength between them and decreases the wear rate [22].

3.4 Wear surface morphology

Figure 10 indicates the surface morphology of composite samples after wear testing. According to Figure 10, the wear rate of samples decreases at a higher number of cycles. Also, small wear tracks are the result of abrasive wear mechanisms (Figure 10). Finally, the result shows that the composite samples reinforced with 10% alumina particles have better wear resistance properties in comparison with monolithic samples. Based on the abovementioned discussions and after the beginning of wear, growth of the grains occurred at the plastically deformed region (between the pin and the worn surface) due to high temperature. So, a coarse grain structure is formed under subsurface which had a strain incompatibility regarding the fine grain structure and non-equilibrium

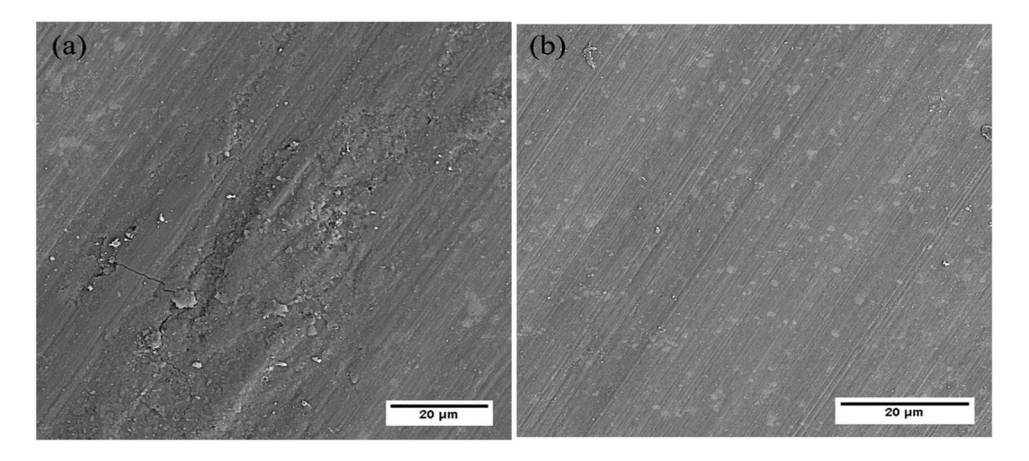


Figure 10: Wear surface of the (a) monolithic and (b) Al/10 Vol% alumina composites.

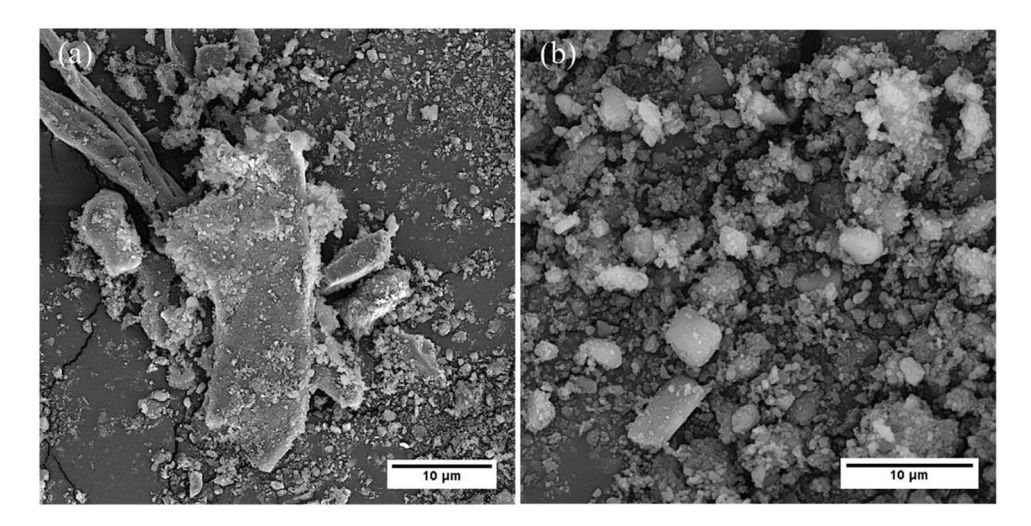


Figure 11: SEM micrographs of wear debris particles of (a) monolithic and (b) composite reinforced with 10 Vol% of alumina.

ultrafine grains. In the other words, debris particles were formed when the strain incompatibility caused delamination of coarse grains as the subsurface of the wearing samples. Increasing the alumina Vol% decreases the width of wear groves and improves the wear resistance due to local work hardening of the aluminum matrix around the particles.

Figure 11 shows the SEM image of debris after the wear test of monolithic and composite samples fabricated with 10 Vol% of alumina particles. As mentioned before

according to Figure 12, after the beginning of the wear between the worn surfaces and pin, growth of the grains occurred due to high temperature in the plastically deformed region with more growth in the subsurface zone than the middle thickness. So, under subsurface which had a strain incompatibility regarding the fine grain structure and non-equilibrium ultrafine grains a coarse grain structure is formed. In the other words when the strain incompatibility caused delamination of coarse grains as the subsurface of the wearing samples, debris particles were formed.

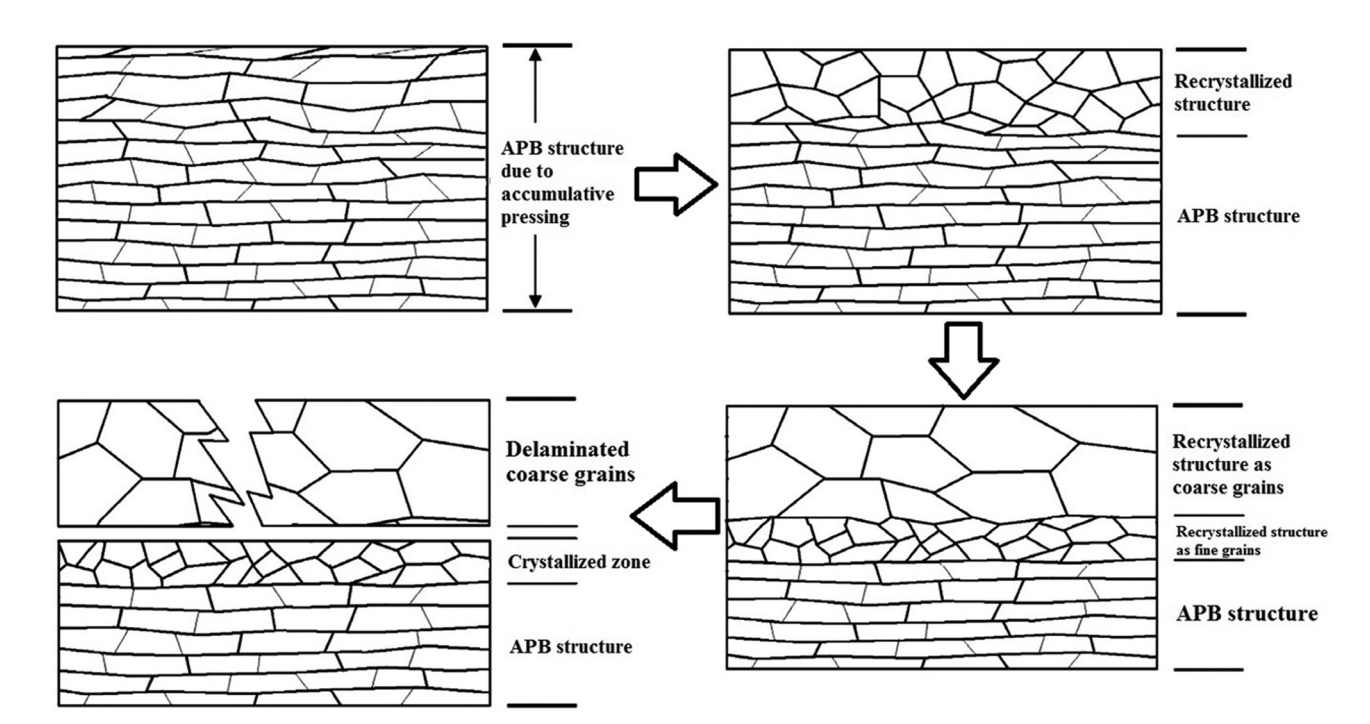


Figure 12: Schematics of the sliding wear of ARB composite samples vs different steps of deformation and recrystallization mechanism.

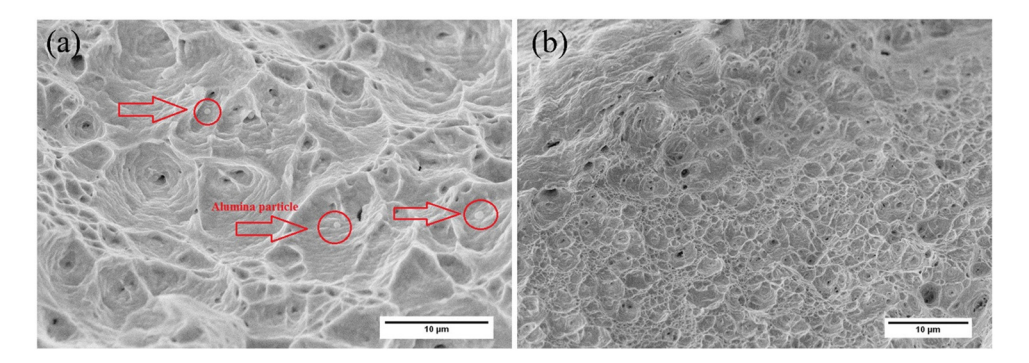


Figure 13: Rapture morphology of (a) monolithic and (b) Al/10 Vol% alumina.

Also, these delamination and recrystallization processes occurred in repetitive rounds. Always, the generation of large particle debris in a shape is the result of this kind of wear mechanism. The initiation and nucleation of cracks on the sliding surfaces are the results of high shear stresses. So, this changes the shape of the loss of material from flakes to plates. So, the flows of surface material are toward the sliding direction which generates abrasive grooves under a higher applied load [28–30]. The debris size for the sample fabricated with 10% alumina content is less than that of the monolithic sample. This difference in the size of debris is the result of the local strengthening mechanism around the alumina particles which creates localized hardened regions around the alumina particles. Then, as a result, the size of debris decreases.

3.5 Fractography

To clarify the rupture mechanisms in the monolithic and Al/10 vol% alumina composite samples, an SEM study is conducted (Figure 13). Typically shear regions and deep dimples of the monolithic sample are the results of typically ductile fracture (Figure 13(a)). This type of rapture mode happens through the coalescence and formation of voids. By increasing the alumina content, the length of dimples decreases which has a particular effect on the fracture surface. Alumina substances sit on the cores and walls of dimples and are suitable sites for the propagation of micro-cracks [21,31,35,36].

4 Conclusions

At this point, the new AMMCs are made through four cycles of the ARB process by diffusing Al₂O₃ volume content particles, the Phase conformation, mechanical properties and wear resistance of these kinds of composites, and

microstructure properties were scrutinized. In summary, the following conclusions were drawn:

- Fairly constant scattering of particulates in the Al matrix released by scanning electron microscopy. The strength, tensile toughness, and wear resistance of composites were enhanced due to the addition of alumina particles.
- 2. The results revealed that the composites with 10 Vol% of alumina particulates have better wear resistance properties compared to the monolithic sample.
- 3. Increasing alumina Vol% enhances the strength of composites. So, it reaches a maximum value of 178 MPa with 10 Vol% of alumina particles which is about 1.40 times more than that of monolithic composite.
- 4. The elongation for the composite sample fabricated via 10 Vol% of alumina was 1.79 and for the monolithic sample was 4.28 registering about 2.39 times decrease.
- 5. The average Vickers hardness amount of the samples improves from 157.0 to 167.0 for monolithic and 10% alumina samples registering a 5.7% improvement, respectively.

Acknowledgments: The authors gratefully acknowledge the Nanyang Normal University and Majlesi branch of Islamic Azad University manufacturing technology research center for the provision of experimental set up and research facilities used in this work.

Funding information: The authors would like to thank the support from the National Science Foundation Incubation Youth Project of Nanyang Normal University (2022PY020) and Natural Science Youth Foundation of Nanyang Normal University (2020QN037).

Author contributions: Yuanfei Gao, Mohammad Heydari Vini and Saeed Daneshmand conceived of the presented idea. Yuanfei Gao supplied the results for answering the revision and supported the experimental parts. M.

Heydari Vini designed the experiments and conducted the approaches and Saeed Daneshmand classified the results and wrote the article text. All authors discussed the results and contributed to the final manuscript.

Conflict of interest: No potential conflict of interest was reported by the author(s).

Data availability statement: The data that support the findings of this study are openly available in [repository name e.g, "figshare"] http://doi.org/[doi], reference number [reference number].

References

- Meselhy, A. F. and A. F. Meselhy. Investigation of mechanical properties of nanostructured Al-SiC composite manufactured by accumulative roll bonding. Composite Materials, Vol. 53, 2019, pp. 28-30.
- Medhat Elwan, A. and A. Fathy. Wagih, Fabrication and investigation on the properties of ilmenite (FeTiO3)-based Al composite by accumulative roll bonding. Journal of Composite Materials, Vol. 54, No. 10, 2019, pp. 1259-1271.
- [3] El Mahallawy, N., A. Fathy, M. Hassan, and W. Abdelaziem. Evaluation of mechanical properties and microstructure of Al/Al-12%Si multilayer via warm accumulative roll bonding process. Journal of Composite Materials, Vol. 54, 2017, id. 0021998317692141. doi: 10.1177/0021998317692141.
- [4] Sadoun, A. M., M. M. Mohammed, A. Fathy, and O. A. El-Kady. Effect of Al₂O₃ addition on hardness and wear behavior of Cu-Al₂O₃ electro-less coated Ag nanocomposite. Journal of Materials Research and Technology, Vol. 9, No. 3, 2020, nn. 5024-5033.
- [5] Sadoun, A. M., M. M. Mohammed, E. M. Elsayed, A. F. Meselhy, and O. A. El-Kady. Effect of nano Al₂O₃ coated Ag addition on the corrosion resistance and electrochemical behavior of Cu-Al₂O₃ nanocomposites. Journal of Materials Research and Technology, Vol. 9, No. 3, 2020, pp. 4485-4493.
- Mohammed, M. M., A. F. Ibrahim, and O. A. El-Kady. Effect of nano Al₂O₃ coated Ag reinforced Cu matrix nanocomposites on mechanical and tribological behavior synthesis by P/M technique. Composite Materials, Vol. 54, No. 30, 2020, pp. 4921-4928.
- Sadoun, A. M., I. M. R. Najjar, M. S. Abd-Elwahed, and A. Meselhy. Experimental study on properties of Al-Al₂O₃ nanocomposite hybridized by graphene nanosheets. Journal of Materials Research and Technology, Vol. 9, No. 6, 2020, pp. 14708-14717.
- [8] Shaat, M., A. Fathy, and A. Wagih. Correlation between grain boundary evolution and mechanical properties of ultrafinegrained metals. Mechanics of Materials, Vol. 143, 2020,
- [9] Abd-Elwahed, M. S., A. F. Ibrahim, and M. M. Reda. Effects of ZrO₂ nanoparticle content on microstructure and wear

- behavior of titanium matrix composite. Journal of Materials Research and Technology, Vol. 9, No. 4, 2020, pp. 8528-8534.
- [10] Sadoun, A. M., A. F. Meselhy, and A. W. Deabs. Improved strength and ductility of friction stir tailor-welded blanks of base metal AA2024 reinforced with interlayer strip of AA7075. Results in Physics, Vol. 16, 2020, id. 102911.
- [11] Sadoun, A. M., A. Wagih, A. Fathy, and A. R. S. Essa. Effect of tool pin side area ratio on temperature distribution in friction stir welding. Results in Physics, Vol. 15, 2019, id. 102814.
- [12] Megahed, M., A. Fathy, D. Morsy, and F. Shehata. Mechanical performance of glass/epoxy composites enhanced by microand nanosized aluminum particles. Journal of Industrial Textile, Vol. 51, No. 1, 2019, pp. 68-92.
- [13] Sadoun, A. M., F. Abd El-Wadoud, A. Fathy, A. M. Kabeel, and A. A. Megahed. Effect of through-the-thickness position of aluminum wire mesh on the mechanical properties of GFRP/Al hybrid composites. Journal of Materials Research and Technology, Vol. 36, No. 2, 2021, pp. 53-62.
- [14] Xu, R., N. Liang, L. Zhuang, D. Wei, and Y. Zhao. Microstructure and mechanical behaviors of Al/Cu laminated composites fabricated by accumulative roll bonding and intermediate annealing. Materials Science and Engineering, Vol. 832, No. 14, 2022, id. 142510.
- [15] Liu, X., D. Wei, L. Zhuang, C. Cai, and Y. Zhao. Fabrication of high-strength graphene nanosheets/Cu composites by accumulative roll bonding. Materials Science and Engineering: A, Vol. 642, No. 26, 2015, pp. 1-6.
- [16] Chen, Y., J. Nie, F. Wang, H. Yang, C. Wu, X. Liu, et al. Revealing hetero-deformation induced (HDI) stress strengthening effect in laminated Al- $(TiB_2 + TiC)_p/6063$ composites prepared by accumulative roll bonding. Journal of Alloys and Compounds, Vol. 815, 2020, id. 152285.
- [17] Nie, J., M. Liu, F. Wang, Y. Zhao, Y. Li, Y. Cao, et al. Fabrication of Al/Mg/Al composites via accumulative roll bonding and their mechanical properties. Materials, Vol. 9, No. 11, 2016, id. 951.
- [18] Alizadeh, M. and M. Talebian. Fabrication Of Al/Cup composite by accumulative roll bonding process and investigation of mechanical properties. Materials Science and Engineering A, Vol. 558, 2012, pp. 331-337.
- [19] Lu, C., K. Tieu, and D. Wexler. Significant enhancement of bond strength in the accumulative roll bonding process using nanosized Sio₂ particles. J Mater Process Technol, Vol. 209, No. 10, 2009, pp. 4830-4834.
- [20] Alizadeh, M. Comparison of nanostructured Al/B4C composite produced by ARB and Al/B4C composite produced by RRB process. Materials Science & Engineering A, Vol. 528, No. 2, 2010, pp. 578-582.
- [21] Saito, Y., H. Utsunomiya, N. Tsuji, and T. Sakai. Novel ultrahigh straining process for bulk Materials - Development of the accumulative roll-bonding (ARB) process. Acta Materialia, Vol. 47, 1999, pp. 579-583.
- [22] Korbel, A., M. Richert, J. Richert. The effects of very high cumulative deformation on structure and mechanical properties of aluminium. Proceedings of the Second RISO International Symposium on Materials Science, 1981, pp. 14-18.
- [23] Liu, C. Y., Q. Wang, Y. Z. Jia, B. Zhang, R. Jing, M. Z. Ma, et al. Effect of W particles on the properties of accumulatively rollbonded Al/W composites. Materials Science and Engineering A, Vol. 547, 2012, pp. 120-124.

- [24] Liu, C. Y., Q. Wang, Y. Z. Jia, B. Zhang, R. Jing, M. Z. Ma, et al. Evaluation of mechanical properties of 1060-Al reinforced with WC particles via warm accumulative roll bonding process. *Materials and Design*, Vol. 43, 2013, pp. 367–372.
- [25] Ipek, R. Adhesive wear behaviour of B4C and SiC reinforced 4147 Al matrix composites (Al/B4C-Al/SiC). *J Mater Process Technol*, Vol. 162–163, 2005, pp. 71–75.
- [26] Vini, M. H. and S. Daneshmand. Investigation of bonding properties of Al/Cu bimetallic laminates fabricated by the asymmetric roll bonding techniques. *Advances in Computational Design*, Vol. 4, No. 1, 2019, pp. 33–41.
- [27] Amirkhanlou, S., R. Jamaati, B. Niroumand, and M. R. Toroghinejad. Using ARB process as A solution for Dilemma of Si and Sic P Distribution in Cast Al – Si/Sic P composites. *Journal of Materials Processing Technology*, Vol. 211, 2011, pp. 1159–1165.
- [28] Sedighi, M., M. H. Vini, and P. Farhadipour. Effect of alumina content on the mechanical properties of AA5083/Al₂O₃ composites fabricated by warm accumulative roll bonding. *Powder Metallurgy and Metal Ceramics*, Vol. 55, No. 510, 2016, pp. 413–418.
- [29] Su, L., C. Lu, H. Li, G. Deng, and K. Tieu. Investigation of ultrafine grained AA1050 fabricated by accumulative roll bonding. *Materials Science and Engineering A*, Vol. 614, 2014, pp. 148–155.
- [30] Vini, M. H. and M. Sedighi. Mechanical properties and bond strength of bimetallic AA1050/AA5083 laminates fabricated by warm-accumulative roll bonding. *Canadian Metallurgical Quarterly*, Vol. 57, 2019, pp. 160–167.

- [31] Vini, M. H. and S. Daneshmand. Effect of Tio₂ particles on the mechanical, bonding properties and microstructural evolution of AA1060/TiO₂ composites fabricated by WARB. *Advances in Materials Research*, Vol. 9, No. 2, 2020, pp. 99–107.
- [32] Nie, J., F. Wang, Y. Li, Y. Cao, X. Liu, Y. Zhao, et al. Microstructure evolution and mechanical properties of Al-TiB₂/ TiC in situ aluminum-based composites during accumulative roll bonding (ARB) process. *Materials*, Vol. 10, No. 2, 2017, id. 109.
- [33] Jamaati, R. and M. R. Toroghinejad. Manufacturing of highstrength aluminum/alumina composite by accumulative roll bonding. *Materials Science Engineering A*, Vol. 527, No. 16–17, 2010, pp. 4146–4151.
- [34] Heydari Vini, M., M. Sedighi, and M. Mondali. Mechanical properties, bond strength and microstructural evolution of AA1060/TiO₂ composites fabricated by warm accumulative roll bonding (WARB). *Journal of Materials Research*, Vol. 108, No. 1, 2017, pp. 53–59.
- [35] Farhadipour, P., M. Sedighi, and M. Heydari. Using warm accumulative roll bonding method to produce Al-Al₂O₃. Proceedings of the Institution of Mechanical Engineers Part B Journal of Engineering Manufacture, Vol. 231, No. 5, 2017, pp. 889–896.
- [36] Sedighi, M., P. Farhadipour, and M. Heydari Vini. Mechanical properties and microstructural evolution of bimetal 1050/Al₂O₃/5083 composites fabricated by warm accumulative roll bonding. *JOM*, Vol. 68, No. 12, 2016, pp. 3193–3200.